第 35 卷 第 4 期
2018 年 12 月

原 子 核 物 理 评 论
Nuclear Physics Review

Vol. 35, No. 4
Dec., 2018

Article ID: 1007-4627(2018) 04-0523-08

Relativistic Mean-field Approach for Λ, Ξ and Σ Hypernuclei

LIU Zixin[1], XIA Chengjun[2], SUN Tingting[1,†]

(*1. School of Physics and Engineering, Zhengzhou University, Zhengzhou 450001, China;*
2. School of Information Science and Engineering, Ningbo Institute of Technology,
Zhejiang University, Ningbo 315100, Zhejiang, China)

Abstract: Single Λ, Ξ, and Σ hypernuclei are systematically studied within the framework of relativistic mean-field (RMF) model with YN interactions being constrained according to the experimental data and previous theoretical efforts. By adding a hyperon to ^{16}O, the mean-field potentials and single-particle levels for hyperons (Λ, $\Xi^{0,-}$, and $\Sigma^{+,0,-}$) are compared and the impurity effects on the nuclear core are examined. In general, the Λ and Σ^0 hyperons show similar behaviors in bulk properties since both of them are electroneutral and with similar coupling constants; Ξ^0 hyperon owns the shallowest mean-field potential well; and Coulomb interactions play vital roles in the charged Ξ^-, Σ^-, and Σ^+ hyperons. As an impurity, the intruded single-hyperon makes the nuclear system more bound in most cases due to the attractive NY interaction. However, very different effects on the nucleon radii are observed for different hyperons. Besides, the effects of the ωYY tensor couplings on the spin-orbit splitting are discussed, and remarkable influences are found which even change the level ordering of Ξ hyperon.

Key words: hypernuclei; hyperon-nucleon interaction; ωYY tensor coupling; RMF model

CLC number: O571.6 **Document code:** A **DOI:** 10.11804/NuclPhysRev.35.04.523

1 Introduction

Since the first Λ hypernucleus was discovered in 1953[1], the study of hypernuclei has attracted worldwide interests on both experimental observations[2–3] and theoretical calculations[4]. An important goal in hypernuclear physics is to extract information on baryon-baryon interaction, which is crucial to understand the hypernuclear structure[5–6] and neutron star properties[7–9].

Experimentally, many large facilities such as CERN, BNL, JLab, KEK, J-PARC, and MAMI, have been producing a lot of hypernuclei data to investigate the strangeness nuclear physics[2–3]. So far, the single-Λ hypernuclei are most extensively studied and more than 30 events ranging from $^{3}_{\Lambda}$H to $^{208}_{\Lambda}$Pb have been obtained in laboratories[2]. However, almost no bound Σ-hypernuclear systems are observed except for $^{4}_{\Sigma}$He, which was produced in the (K^-_{stop}, π^-) reaction at KEK[10]. For the S=−2 hypernuclei, the experimental data are also very limited. Until now, three double-Λ hypernuclei $^{6}_{\Lambda\Lambda}$He[11], $^{10}_{\Lambda\Lambda}$Be[12], and $^{13}_{\Lambda\Lambda}$Be[13] have been identified and the observed positive ΛΛ bond energies $\Delta B_{\Lambda\Lambda} = B_{\Lambda\Lambda} - 2B_{\Lambda}$ suggest slightly attractive ΛΛ interaction. Meanwhile, there are only several observed data on the Ξ hypernuclei in the $^{12}_{\Xi}$Be (^{11}B + Ξ^-)[14], $^{13}_{\Xi}$B (^{12}C + Ξ^-)[15], and $^{15}_{\Xi}$C (^{14}N + Ξ^-)[16] systems. Especially, the Kiso event with the process of Ξ^- + ^{14}N → $^{10}_{\Lambda}$Be + $^{5}_{\Lambda}$He provided the first clear evidence of a deeply bound state of the Ξ^--^{14}N system by an attractive ΞN interaction[16].

Theoretically, great efforts have been made with various models to study the hypernuclei as a many-body system. As impurities, the hyperons may induce many effects on the nuclear core, such as the shrinkage effect[17–18], deformation[19–20], modification of cluster structure[21], shift of neutron drip line[22], halo structures[23] and spin and pseudospin symmetries[24–27]. Many approaches such as the cluster model[17, 28], the shell model[29–30], the anti-symmetrized molecular dynamics[31], the mean-field approaches[19–20, 32–35], quark mean-field model[8], and *ab initio* methods[36] have contributed a lot on the investigations of the structure of hypernuclei and obtained great successes. Among these theoretical methods, the mean-field approaches can be globally applied

Received date: 23 Sep. 2018; **Revised date:** 3 Nov. 2018

Foundation item: National Natural Science Foundation of China (11505157, 11705163); Physics Research and Development Program of Zhengzhou University (32410017)

Biography: LIU Zixin(1994–), male, Changsha, Hunan, Master, working on nuclear physics;

† **Corresponding author:** SUN Tingting, E-mail: ttsunphy@zzu.edu.cn.

from light to heavy hypernuclei, like Skyrme-Hartree-Fock (SHF)[19] and the relativistic mean-field (RMF) models[20, 32–35].

During the past decades, the RMF model was very successful on describing the properties of ordinary nuclei[37–39]. In 1977, Brockmann and Weise first applied this approach to hypernuclei with the strangeness degree of freedom[32]. At that time, it had been already observed experimentally that the spin-orbit splittings in hypernuclei are significantly smaller than those in ordinary nuclei[40]. The relativistic approach is suitable for a discussion of spin-orbit splittings, which is naturally emerged within the relativistic framework. As a result, the RMF model has been applied to describe single- and multi-Λ systems, including the single-particle (s.p.) spectra of Λ-hypernuclei and the spin-orbit splittings, and extended beyond the Λ hyperon to other strangeness baryons.

In this work, we aim to investigate the properties of single-Λ, Ξ, and Σ hypernuclei systematically within the framework of RMF model. Proper YN interactions will be adopted. Similar investigations for single-hyperon hypernuclei by RMF model can be seen in Refs. [33, 35]. The paper is organized as follows. In Sec. 2, we present the RMF model for the single-Λ, Σ, and Ξ hypernuclei. After the numerical details in Sec. 3, we present the results and discussions in Sec. 4. Finally, a summary is drawn in Sec. 5.

2 Theoretical framework

The Lagrangian density of the meson-exchange RMF model for hypernuclei is

$$\mathcal{L}=\mathcal{L}_{\rm N}+\mathcal{L}_{\rm Y}, \tag{1}$$

where $\mathcal{L}_{\rm N}$ is for the nucleons[37–38], and $\mathcal{L}_{\rm Y}$ is the contribution from the hyperons. For the electroneutral Λ hyperon with isospin 0, only the couplings with σ and ω mesons are included; and for the Ξ and Σ hyperons, the couplings with σ, ω, and ρ mesons and photon are included. The Lagrangian density $\mathcal{L}_{\rm Y}$ reads[33, 35],

$$\begin{aligned}\mathcal{L}_{\rm Y}=&\bar{\psi}_{\rm Y}\Big[{\rm i}\gamma^{\mu}\partial_{\mu}-M_{\rm Y}-g_{\sigma{\rm Y}}\sigma-g_{\omega{\rm Y}}\gamma^{\mu}\omega_{\mu}-\\&\frac{f_{\omega{\rm Y}}}{2M_{\rm Y}}\sigma^{\mu\nu}\partial_{\nu}\omega_{\mu}\Big]\psi_{\rm Y}+\mathcal{L}_{\rho{\rm Y}}+\mathcal{L}_{\rm AY},\end{aligned} \tag{2}$$

where $M_{\rm Y}$ are the hyperon masses, $g_{\sigma{\rm Y}}$, $g_{\omega{\rm Y}}$, and $g_{\rho{\rm Y}}$ are the coupling constants with the σ, ω, and ρ mesons, respectively, and the term proportional to $\frac{f_{\omega{\rm Y}}}{2M_{\rm Y}}$ represents the tensor coupling with the ω field. The two terms $\mathcal{L}_{\rho{\rm Y}}$ and $\mathcal{L}_{\rm AY}$ describe the couplings with the ρ meson and Coulomb field, which should be included for the Ξ and Σ hypernuclei. For a particular hyperon, they read,

$$\mathcal{L}_{\rho{\rm Y}}=\begin{cases}0, & \text{for } \Lambda,\\ -\bar{\psi}_{\Xi}g_{\rho\Xi}\gamma^{\mu}\boldsymbol{\tau}_{\Xi}\cdot\boldsymbol{\rho}_{\mu}\psi_{\Xi}, & \text{for } \Xi,\\ -\bar{\psi}_{\Sigma}g_{\rho\Sigma}\gamma^{\mu}\boldsymbol{\tau}_{\Sigma}\cdot\boldsymbol{\rho}_{\mu}\psi_{\Sigma}, & \text{for } \Sigma,\end{cases} \tag{3}$$

and

$$\mathcal{L}_{\rm AY}=\begin{cases}0, & \text{for } \Lambda,\\ -\bar{\psi}_{\Xi}e\gamma^{\mu}\dfrac{\tau_{\Xi,3}-1}{2}A_{\mu}\psi_{\Xi}, & \text{for } \Xi,\\ -\bar{\psi}_{\Sigma}e\gamma^{\mu}\tau_{\Sigma,3}A_{\mu}\psi_{\Sigma}, & \text{for } \Sigma,\end{cases} \tag{4}$$

where $\boldsymbol{\rho}_{\rm Y}$ is the isospin vector with the third component $\tau_{{\rm Y},3}$,

$$\tau_{{\rm Y},3}=\begin{cases}0, & {\rm Y}=\Lambda,\\ +1,\ -1, & {\rm Y}=\Xi^0,\ \Xi^-,\\ +1,\ 0,\ -1, & {\rm Y}=\Sigma^+,\ \Sigma^0,\ \Sigma^-.\end{cases} \tag{5}$$

For a system with time-reversal symmetry, the space-like components of the vector fields vanish, leaving only the time components ω_0, $\boldsymbol{\rho}_0$, and A_0. Furthermore, one can assume that the hyperon s.p. states do not mix isospin, *i.e.*, the s.p. states are eigenstates of $\tau_{{\rm Y},3}$, and therefore only the third component of the $\boldsymbol{\rho}_0$ meson field, $\rho_{0,3}$, survives.

With the mean-field and no-sea approximations, the s.p. Dirac equations for baryons and the Klein-Gordon equations for mesons and photon can be obtained by the variational procedure. In the spherical case, the Dirac spinor can be expanded as

$$\psi(\boldsymbol{r})=\frac{1}{r}\begin{pmatrix}{\rm i}G_{n\kappa}(r)\\ F_{\tilde{n}\kappa}(r)\ \boldsymbol{\sigma}\cdot\hat{\boldsymbol{r}}\end{pmatrix}Y^{l}_{jm}(\theta,\phi), \tag{6}$$

where $G_{n\kappa}(r)/r$ and $F_{\tilde{n}\kappa}(r)/r$ are the radial wave functions for the upper and lower components with n and $\tilde{n}$ numbers of radial nodes, $Y^{l}_{jm}(\theta,\phi)$ is the spinor spherical harmonics, quantum number κ is defined by the angular momenta (l,j) as $\kappa=(-1)^{j+l+1/2}(j+1/2)$.

The Dirac equation for the radial wave functions of the hyperon is

$$\begin{pmatrix}V+S & -\dfrac{\rm d}{{\rm d}r}+\dfrac{\kappa}{r}+T\\ \dfrac{\rm d}{{\rm d}r}+\dfrac{\kappa}{r}+T & V-S-2M_{\rm Y}\end{pmatrix}\begin{pmatrix}G\\F\end{pmatrix}=\varepsilon\begin{pmatrix}G\\F\end{pmatrix}, \tag{7}$$

where ε is the s.p. energy. For a particular hyperon, the scalar potential S, vector potential V, and ωYY tensor potential T are

$$S=g_{\sigma{\rm Y}}\sigma,\quad \text{for } \Lambda,\ \Xi\ \text{ or }\ \Sigma, \tag{8a}$$

$$V=\begin{cases} g_{\omega\Lambda}\omega_0, & \text{for } \Lambda, \\ g_{\omega\Xi}\omega_0+g_{\rho\Xi}\tau_{\Xi,3}\rho_{0,3}+e\dfrac{\tau_{\Xi,3}-1}{2}A_0, & \text{for } \Xi, \\ g_{\omega\Sigma}\omega_0+g_{\rho\Sigma}\tau_{\Sigma,3}\rho_{0,3}+e\tau_{\Sigma,3}A_0, & \text{for } \Sigma, \end{cases} \tag{8b}$$

and

$$T=-\frac{f_{\omega\mathrm{Y}}}{2M_{\mathrm{Y}}}\partial_r\omega_0, \quad \text{for } \Lambda,\ \Xi \text{ or } \Sigma. \tag{8c}$$

With the radial wave functions, densities in the RMF model for the hyperons can be expressed as

$$\rho_{s\mathrm{Y}}(r)=\frac{1}{4\pi r^2}\sum_{k=1}^{A_{\mathrm{Y}}}\left[|G_k^{\mathrm{Y}}(r)|^2-|F_k^{\mathrm{Y}}(r)|^2\right], \tag{9a}$$

$$\rho_{v\mathrm{Y}}(r)=\frac{1}{4\pi r^2}\sum_{k=1}^{A_{\mathrm{Y}}}\left[|G_k^{\mathrm{Y}}(r)|^2+|F_k^{\mathrm{Y}}(r)|^2\right], \tag{9b}$$

$$j^{0i}_{\mathrm{TY}}(r)=\frac{1}{4\pi r^2}\sum_{k=1}^{A_{\mathrm{Y}}}\left[2G_k^{\mathrm{Y}}(r)F_k^{\mathrm{Y}}(r)\right]\boldsymbol{n}, \tag{9c}$$

$$\rho_{3\mathrm{Y}}(r)=\frac{1}{4\pi r^2}\sum_{k=1}^{A_{\mathrm{Y}}}\left[|G_k^{\mathrm{Y}}(r)|^2+|F_k^{\mathrm{Y}}(r)|^2\right]\tau_{\mathrm{Y},3}; \tag{9d}$$

and

$$\rho_{c\mathrm{Y}}(r)=\begin{cases} \dfrac{1}{4\pi r^2}\displaystyle\sum_{k=1}^{A_\Xi}\left[|G_k^{\Xi}(r)|^2+|F_k^{\Xi}(r)|^2\right]\frac{\tau_{\Xi,3}-1}{2}, & \text{for } \Xi; \\ \dfrac{1}{4\pi r^2}\displaystyle\sum_{k=1}^{A_\Sigma}\left[|G_k^{\Sigma}(r)|^2+|F_k^{\Sigma}(r)|^2\right]\tau_{\Sigma,3}, & \text{for } \Sigma, \end{cases} \tag{9e}$$

where $\boldsymbol{n}$ is the angular unit vector. The hyperon number A_{Y} is determined by the baryon density $\rho_{v\mathrm{Y}}(r)$ as

$$A_{\mathrm{Y}}=\int 4\pi r^2\mathrm{d}r\rho_{v\mathrm{Y}}(r). \tag{10}$$

The coupled Eqs. (7)∼(9) in the RMF model are solved by iteration in the coordinate space.

3 Numerical details

In this work, the single-Λ, Σ, and Ξ hypernuclei are studied by the RMF model. For the NN interaction, the effective interaction PK1[41] is adopted, which can provide excellent descriptions not only for nuclear matter but also for finite nuclei both in and far from the valley of β stability. For the YN interaction, the sets of coupling constants $\alpha_{\sigma\mathrm{Y}}=g_{\sigma\mathrm{Y}}/g_{\sigma\mathrm{N}}$, $\alpha_{\omega\mathrm{Y}}=g_{\omega\mathrm{Y}}/g_{\omega\mathrm{N}}$, $\alpha_{\rho\mathrm{Y}}=g_{\rho\mathrm{Y}}/g_{\rho\mathrm{N}}$, and $\alpha_{\mathrm{TY}}=f_{\omega\mathrm{Y}}/g_{\omega\mathrm{Y}}$ are listed in Table 1.

Table 1　Coupling constants $\alpha_{\sigma\mathrm{Y}}=g_{\sigma\mathrm{Y}}/g_{\sigma\mathrm{N}}$, $\alpha_{\omega\mathrm{Y}}=g_{\omega\mathrm{Y}}/g_{\omega\mathrm{N}}$, $\alpha_{\rho\mathrm{Y}}=g_{\rho\mathrm{Y}}/g_{\rho\mathrm{N}}$, and $\alpha_{\mathrm{TY}}=f_{\omega\mathrm{Y}}/g_{\omega\mathrm{Y}}$ in the YN interactions.

	$\alpha_{\sigma\mathrm{Y}}$	$\alpha_{\omega\mathrm{Y}}$	$\alpha_{\rho Y}$	α_{TY}			
Λ	0.618	0.667	0.0	0.0	−0.122	−0.541	−1.0
Ξ	0.313	0.333	1.0	0.0	−0.4	−1.89	−2.27
Σ	0.619	0.667	1.0	0.0	0.76	1.0	1.417

For the scalar coupling constants, the ΛN interaction is taken as in Ref. [26], which is fixed by reproducing the experimental single-Λ binding energy $B_\Lambda^{(1s)}$ of the $1s$ orbit in hypernucleus ${}^{40}_{\Lambda}$Ca. With this ΛN parameter, the single-Λ spectra for hypernuclei from ${}^{12}_{\Lambda}$C to ${}^{208}_{\Lambda}$Pb can be well described. The ΞN interaction is taken as in Ref. [42], which is determined by fitting the observed Ξ^- removal energy in the Kiso event related to the hypernucleus ${}^{15}_{\Xi}$C (^{14}N+Ξ^-). For the ΣN interaction, due to the insufficient experimental information, the coupling constants between Σ hyperons and mesons still have a lot of ambiguities. In Ref. [43], to study the neutron star maximum masses, the ΣN interaction is taken to be repulsive and the coupling constants are determined by fitting the empirical hyperon-nucleon potentials $U_\Sigma^{(\mathrm{N})}=0,+30$ MeV at nuclear saturation density. However, by comparing the binding energy of Σ hyperon $B_\Sigma=3.2\pm$ MeV[10] or $=4.4\pm0.3$ (stat) ±1(syst) MeV[44] in ${}^{4}_{\Sigma}$He with that for Λ hyperon $B_\Lambda=2.39\pm0.03$ MeV in ${}^{4}_{\Lambda}$He[3], the Σ hyperons are more bound. Thus, we take the ΣN interaction as in Ref. [33], where $g_{\sigma\Sigma}$ is obtained by the estimated Σ potential $U_\Sigma^{(\mathrm{N})}=-20\sim-30$ MeV in nuclear matter.

In these YN interactions, the vector coupling constants $g_{\omega\mathrm{Y}}$ are taken according to the naive quark model[45], namely,

$$g_{\omega\Lambda}=g_{\omega\Sigma}=2g_{\omega\Xi}=\frac{2}{3}g_{\omega\mathrm{N}}, \tag{11}$$

and the tensor coupling constants α_{TY} are adopted as $\alpha_{\mathrm{T}\Lambda}$=−1.0[26], $\alpha_{\mathrm{T}\Xi}$=−0.4[46], and $\alpha_{\mathrm{T}\Sigma}$=1.0[45], respectively. Several other values of α_{TY}, *i.e.*, $\alpha_{\mathrm{T}\Lambda}$=−0.122, −0.541, $\alpha_{\mathrm{T}\Xi}$=−1.89, −2.27, and $\alpha_{\mathrm{T}\Sigma}=0.76,1.417$[33] are also taken to investigate the ωYY tensor coupling effects on the s.p. levels.

The equations in RMF model are solved in the coordinate space with a box size of $R=20$ fm and a step size of 0.1 fm.

4 Results and discussion

In Fig. 1, the hyperon mean-field potentials $V+S$ and the corresponding s.p. levels in the hypernuclei ^{16}O+Y are presented, where Y= Λ, $\Xi^{0,-}$, and $\Sigma^{+,0,-}$. For comparison, we first set the ωYY tensor coupling constant $\alpha_{\mathrm{TY}}=0$ for all hypernuclei. Obvious differences in the potential depths are obtained except for the Λ and Σ^0 hyperons, with very similar mean-field potentials indicated by solid lines. This is because that both the Λ and Σ^0 hyperons couple only with σ and ω mesons and have very close coupling strengths as shown in Table 1. Moreover, in panel (a), the potential depth of the Λ hyperon is about twice

of the Ξ^0 hyperon, which yields fewer bound states in the Ξ^0 spectra. This is mainly due to the weaker σ-Ξ^0 and ω-Ξ^0 couplings, which are around half of σ-Λ and ω-Λ couplings. However, the Ξ^- hyperon is more deeply bound than the Ξ^0 hyperon, which is caused by the attractive Coulomb potential of Ξ^- hyperons. In panel (b), the results of Σ hyperons are presented. The effect of Coulomb interaction is very distinct. From Σ^- to Σ^+ hypernuclei, the s.p. states become almost 11 MeV less bound, and the Coulomb barrier around 2 MeV near the nuclear surface of the Σ^+ can be seen clearly.

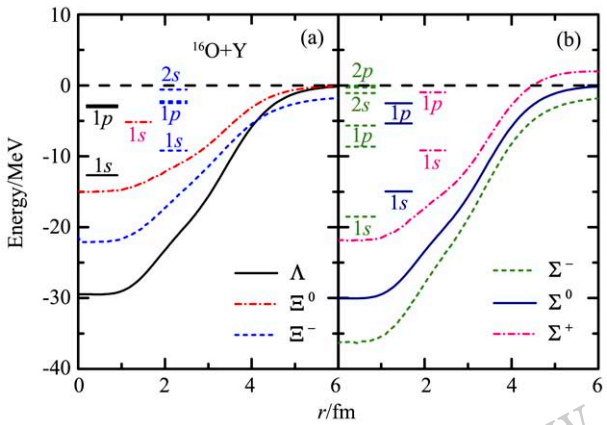

Fig. 1 (color online) Mean-field potentials $V+S$ and s.p. levels for the hyperons in the hypernuclei ^{16}O+Y. In panel (a), Y= Λ and $\Xi^{0,-}$, and in panel (b), Y=$\Sigma^{+,0,-}$. $\alpha_{\rm TY}=0$.

To understand the differences in the mean-field potentials for hyperons, in Fig. 2, we show the various contributions. In Fig. 2(a), for the Λ hyperon, only σ and ω mesons contribute to the total potential. In Fig. 2(b) and (c), for the Ξ^- and Σ^- hyperons, besides the σ and ω mesons, the ρ meson and photons also contribute to the total potentials. However, in the RMF calculations of the single Ξ or Σ hypernuclei ^{16}O+Y with a pure isospin-zero nuclear core, the entire ρ field is generated by the hyperon self-interaction, which is considered as "spurious" and should be removed. In the following, as in Ref. [33], we isolate the Y-ρ self-interaction in Ξ and Σ hypernuclei by switching off the ρ coupling to the nucleons, while the Y-ρ interaction is left unchanged. By comparing the results with those for $g_{\rho\rm N}=g_{\rho\rm Y}=0$, we obtain the spurious contribution of the hyperon self-interaction, which we then subtract from the results of the full calculation.

In Fig. 2, the contributions from $V_{\sigma+\omega}$ are very close for the Λ and Σ^- hyperons, but much larger than that for the Ξ^- hyperon, due to the smaller σ-Ξ and ω-Ξ couplings. Meanwhile, the potential $V_{\sigma+\omega}$ leads to the main difference of $V_{\rm tot}$ between the Ξ^- and Σ^- hyperons. The contributions from Coulomb potential $V_{\rm cou}$ are quite similar for these negative charged hyperons. For the contributions from ρ meson, the spurious potential $V_\rho^{(\rm S)}$ is repulsive and around 4.2 MeV and 5.6 MeV in the central part for the Ξ^- and Σ^- hyperon, respectively. However, the potential V_ρ contributed by the ρ meson is much reduced after subtracting $V_\rho^{(\rm S)}$ and becomes slightly attractive. Potentials V_ρ are attractive for the Ξ^- and Σ^- hyperons with $\tau_{\rm Y,3}=-1$ while repulsive for the Ξ^0 and Σ^+ hyperons with $\tau_{\rm Y,3}=+1$. Although the magnitude of V_ρ is much smaller than that of $V_\rho^{(\rm S)}$, it is not negligible and represents the effect of ρ meson in the hypernuclei

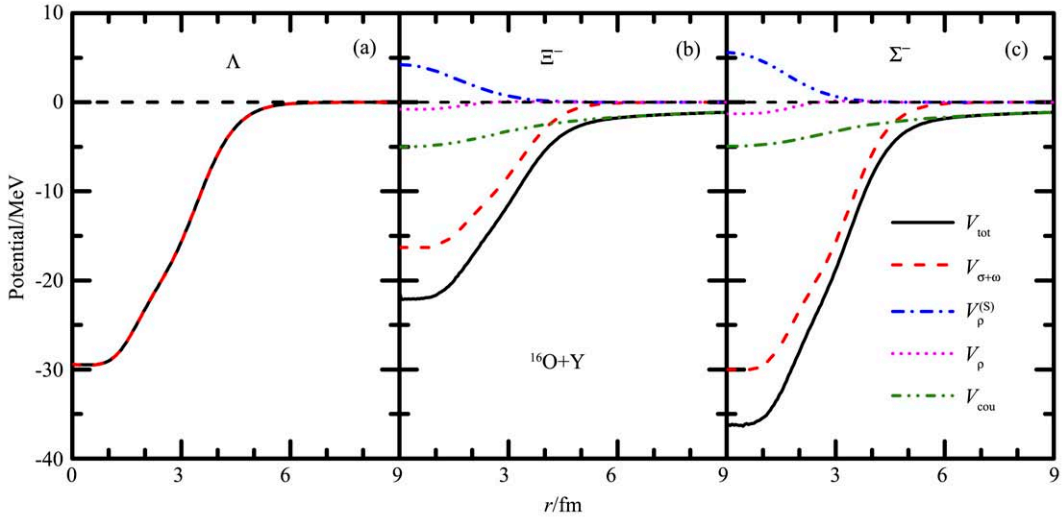

Fig. 2 (color online) Comparison of the total mean-field potential $V_{\rm tot}=V_{\sigma+\omega}+V_\rho+V_{\rm cou}$ (solid curves) and various distributions (dashed curves) from the σ, ω, and ρ mesons, and photons for the Y=Λ (a), Ξ^- (b) and Σ^- (c) hyperons in the hypernuclei ^{16}O+Y. Spurious potentials $V_\rho^{(\rm S)}$ corresponding to hyperon self-coupling interactions are also presented for Ξ^- and Σ^- hypernuclei. $\alpha_{\rm TY}=0$.

with an isospin saturated nuclear core[33].

Since hyperons do not suffer from the nucleon's Pauli exclusion principle, there will be a series of responses for the nuclear core if any hyperons penetrate into the nuclear interior as an impurity. In Table 2, to study the hyperon impurity effects, various energies and radii are listed for the ordinary nucleus ^{16}O and the single-hyperon hypernuclei $^{17}_{\Lambda}$O (^{16}O+Λ), $^{17}_{\Xi^0}$O ($^{16}\mathrm{O}+\Xi^0$), $^{17}_{\Xi^-}$N ($^{16}\mathrm{O}+\Xi^-$), $^{17}_{\Sigma^+}$F ($^{16}\mathrm{O}+\Sigma^+$), $^{17}_{\Sigma^0}$O ($^{16}\mathrm{O}+\Sigma^0$), and $^{17}_{\Sigma^-}$N ($^{16}\mathrm{O}+\Sigma^-$). By comparing the total binding energies $E_{\rm tot}$ between ^{16}O and single-hyperon hypernuclei, it can be easily seen that the added hyperon makes the nuclear systems much more bound due to the attractive NY interactions, especially in the hypernuclei $^{17}_{\Lambda}$O, $^{17}_{\Sigma^0}$O, and $^{17}_{\Sigma^-}$N. The energy differences mainly come from the single-hyperon energies $\varepsilon^{\rm Y}_{1s}$, which are larger for the Λ, Σ^0, and Σ^- hyperons. The c.m. correction $E_{\rm c.m.}$ in different hypernuclei are very close, and their slight differences may be due to the hyperon mass difference. Removing $\varepsilon^{\rm Y}_{1s}$ and $E_{\rm c.m.}$ from the total binding energy, the energy contributed by the nuclear core can be described, *i.e.*, $E_{\rm core}=E_{\rm tot}-\varepsilon^{\rm Y}_{1s}-E_{\rm c.m.}$, which are found very close with the difference less than 0.65 MeV.

Table 2　Energies (in MeV) and radii (in fm) for the single hyperon hypernuclei ^{16}O+Y with Y=Λ, $\Xi^{0,-}$, and $\Sigma^{+,0,-}$ and ordinary nucleus ^{16}O by the RMF model. Energies listed are, respectively, the total binding energy $E_{\rm tot}$, the hyperon s.p. energy of $1s_{1/2}$ orbit $\varepsilon^{\rm Y}_{1s}$, energy contributed by the nuclear core $E_{\rm core}$, and the c.m. correction $E_{\rm c.m.}$. Detailed contributions for the hyperon energy from the σ, ω, and ρ mesons and Coulomb force are presented as well, *i.e.*, $E_{\sigma Y}=\int 4\pi r^2 {\rm d}r g_{\sigma Y}\rho_{sY}\sigma$, $E_{\omega Y}=\int 4\pi r^2{\rm d}r[g_{\omega Y}\rho_{vY}\omega_0+\frac{f_{\omega Y}}{2m_Y}\partial_i j^{0i}_{\rm TY}\omega_0]$, $E_{\rho Y}=\int 4\pi r^2{\rm d}r g_{\rho Y}\rho_{3Y}\rho_{0,3}$, and $E^{\rm Y}_{\rm cou}=\int 4\pi r^2{\rm d}r e\rho_{cY}A_0$. Radii listed are, respectively, the mass radius $R_{\rm tot}$, hyperon radius $R_{\rm Y}$, neutron radius $R_{\rm n}$, and proton radius $R_{\rm p}$, calculated by $R=\sqrt{\int {\rm d}r r^4\rho_v(r)/\int {\rm d}r r^2\rho_v(r)}$ with the particle vector density $\rho_v(r)$ and charge radius $R_{\rm c}$ calculated by $R_{\rm c}=\sqrt{R^2_{\rm p}+0.864^2+0.336^2\times\frac{N}{Z}}$. $\alpha_{\rm T\Lambda}=-1$, $\alpha_{\rm T\Xi}=-0.4$, and $\alpha_{\rm T\Sigma}=1$.

	^{16}O	$^{17}_{\Lambda}$O	$^{17}_{\Xi^0}$O	$^{17}_{\Xi^-}$N	$^{17}_{\Sigma^+}$F	$^{17}_{\Sigma^0}$O	$^{17}_{\Sigma^-}$N
$E_{\rm tot}$	−128.101	−140.345	−132.911	−136.955	−137.411	−142.646	−146.499
$\varepsilon^{\rm Y}_{1s}$		−12.673	−5.182	−9.191	−9.165	−14.946	−18.511
$E_{\rm core}$	−117.281	−117.138	−117.426	−117.367	-117.785	−117.148	−117.396
$E_{\rm c.m.}$	−10.820	−10.533	−10.303	−10.397	−10.461	−10.552	−10.592
$E_{\sigma Y}$		−82.771	35.862	−39.963	−83.399	−90.364	−91.534
$E_{\omega Y}$		73.000	30.929	34.623	73.346	78.845	80.929
$E_{\rho Y}$		0	0.201	−0.120	0.335	0	−0.222
$E^{Y}_{\rm cou}$		0	0	-1.910	2.467	0	−1.992
$R_{\rm tot}$	2.563	2.557	2.580	2.560	2.561	2.553	2.541
$R_{\rm Y}$		2.496	2.845	2.594	2.487	2.318	2.286
$R_{\rm n}$	2.549	2.547	2.523	2.547	2.518	2.546	2.552
$R_{\rm p}$	2.577	2.575	2.602	2.569	2.612	2.572	2.561
$R_{\rm c}$	2.698	2.696	2.722	2.690	2.732	2.695	2.683

To see the detailed energy contributions for the single-hyperon energy $\varepsilon^{\rm Y}_{1s}$, the energies contributed by the σ, ω, ρ mesons and Coulomb field are analyzed. The energy contributions from σ and ω mesons are around -5 MeV ~ -12 MeV while that from ρ meson is much smaller and less than 0.35 MeV. And the Coulomb field contributes remarkable energy around ±2 MeV.

Besides, comparing the mass radii $R_{\rm tot}$ for nucleus ^{16}O and hypernuclei ^{16}O+Y, we find that the hyperon makes the size of the nuclear system smaller in most of the hypernuclear systems, which is in accordance with the conclusion of the larger binding energy $E_{\rm tot}$. The larger mass radius in $^{17}_{\Xi^0}$O than ^{16}O is mainly due to the very weakly bound single-Ξ^0 state, leading to large hyperon radius $R_{\Xi^0}=2.845$ fm. By comparing $R_{\rm n}$, very different impurity effects from the hyperons on the neutron radii are shown, *i.e.*, Ξ^0 and Σ^+ hyperons decrease $R_{\rm n}$, Σ^- hyperons increase $R_{\rm n}$, and Λ, Σ^0, and Ξ^- hyperons have no influences on $R_{\rm n}$. The isospin effect related to the couplings with ρ meson is one reason for those differences. For the hyperons Ξ^0 and Σ^+ with $\tau_{\rm Y,3}=+1$, they make the neutron total mean-field potential deeper, and for the hyperons Ξ^- and Σ^- with $\tau_{\rm Y,3}=-1$, they make the total potential becomes shallower. However, the potentials contributed by ρ mesons are very small after removing the spurious potential $V^{(S)}_{\rho}$. Sometimes, such as in $^{17}_{\Xi^-}$N, the total neutron mean-field potential still becomes deeper. Unlike the case of $R_{\rm n}$, for the proton radius $R_{\rm p}$ and charge radius $R_{\rm c}$, the Coulomb interaction is important, *e.g.*, the positively charged Σ^+ increases $R_{\rm p}$ and R_c while the negatively charged hyperons Ξ^- and Σ^- make them smaller. Besides, the

electroneutral Ξ^0 hyperon increases $R_{\rm p}$ and $R_{\rm c}$ slightly due to the same sign of τ_3 as protons, which leads to a shallower mean-field potential for protons.

In Fig. 3, we study the effects of the ωYY tensor coupling on the hyperon s.p. level and obvious changes in the spin-orbit splittings are found with various ωYY tensor couplings constants $\alpha_{\rm TY}$. For examples, in panel (a), the ωYY coupling reduces the spin-orbit splitting for Λ hyperon obviously; in panels (c), the energy level orders for Ξ^- hyperons change with extremely large negative $\alpha_{\omega\Xi} \leqslant -1.89$; and in panels (d), and (f), the ωYY tensor coupling increases the spin-orbit splitting for the Σ hyperon, which is different from the cases of Λ and Ξ hyperons. The different effects of ωYY tensor couplings on the splittings of Λ, Ξ and Σ can be understood by recasting the Dirac Eq. (7) into a Schrödinger-like equivalent form which we can describe the spin-orbit splitting potential as[27, 33]

$$V_{\rm SO}^{\rm Y} = -\frac{1}{M_{\rm eff}}\left(\frac{1}{M_{\rm eff}}\frac{{\rm d}M_{\rm eff}}{{\rm d}r}+2T\right)\frac{\boldsymbol{l}\cdot\boldsymbol{s}}{r},$$
$$M_{\rm eff} = M_{\rm Y} - \frac{1}{2}(V-S), \tag{12}$$

where the ωYY tensor potential $T = -\frac{\alpha_{\rm TY}}{2M_{\rm Y}} g_{\omega{\rm Y}} \partial_{\rm r}\omega_0$. For the Λ and Ξ hyperons, due to the negative values of $\alpha_{\rm TY}$, the ωYY tensor potential T will decrease the spin-orbit splitting potential $V_{\rm SO}^{\rm Y}$ and lead to smaller spin-orbit splittings. However, for the Σ hyperon, due the positive values of $\alpha_{\rm TY}$, the tensor potential T will increase potential $V_{\rm SO}^{\rm Y}$ and lead to larger spin-orbit splittings.

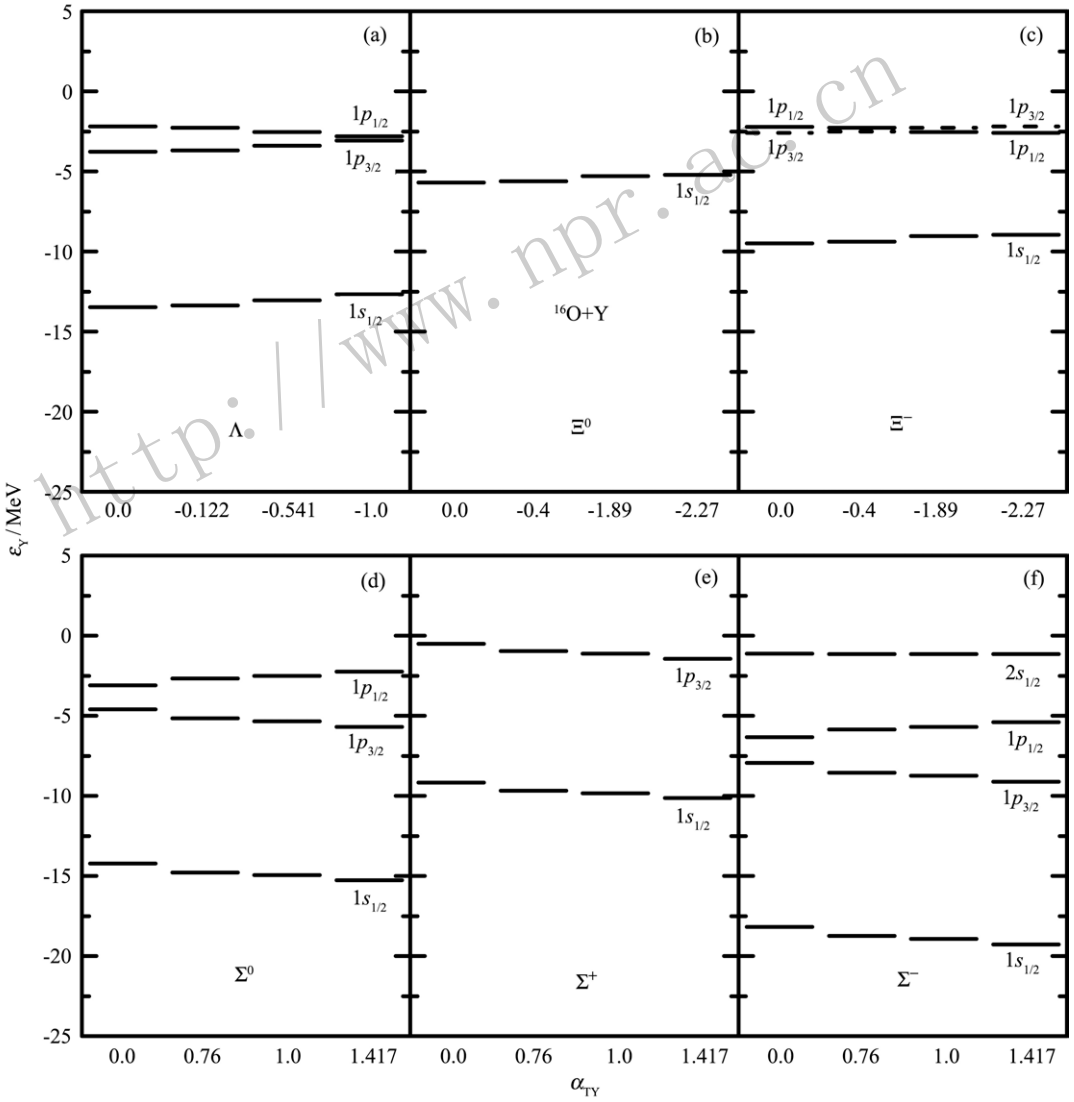

Fig. 3 Positions of the hyperon s.p. levels with different ωYY tensor coupling constants $\alpha_{\rm TY}$ in ^{16}O+Y. The values of $\alpha_{\rm TY}$ are taken as in Table 2. $\alpha_{\rho{\rm Y}} = 0$.

5 Summary

Within the framework of RMF model, the single-hyperon (Y=Λ, $\Xi^{0,-}$, and $\Sigma^{-,0,+}$) hypernuclei are studied systematically. The YN interactions are constrained according to the experimental data or previous theoretical efforts.

Firstly, adding hyperon Y=Λ, $\Xi^{0,-}$, $\Sigma^{+,0,-}$ to nuclear core ^{16}O, the mean-field potentials and single-hyperon levels for different hyperons are investigated. We found that Λ and Σ^0 hyperons have very similar mean-field potentials, the Ξ^0 is the most weakly bound, and Coulomb field plays important roles in the Ξ^-, Σ^-, and Σ^+ hyperons. Besides, the contributions of ρ meson are found very small and they are attractive in Ξ^- and Σ^- hypernuclei while repulsive in Ξ^0 and Σ^0 hypernuclei.

Secondly, the impurity effects from the single-hyperon on the nuclear core are also studied. It is found that the intruded single-hyperon makes the nuclear system more bound in most cases due to the attractive NY interaction. However, very different effects on the nucleon radii are observed for different hyperons. For the neutron radius, Ξ^0 and Σ^+ hyperons decrease $R_{\rm n}$, Σ^- hyperons increase $R_{\rm n}$, and Λ, Σ^0, and Ξ^- hyperons have almost no influences. Unlike the case of R_n, the Coulomb interaction is important for the proton radius $R_{\rm p}$ and charge radius $R_{\rm c}$. The positively charged Σ^+ increase $R_{\rm p}$ and $R_{\rm c}$ while the negatively charged hyperon Ξ^- and Σ^- decrease them.

Finally, the ωYY tensor couplings and the effects on the single-hyperon levels are studied. In general, the ωYY tensor couplings influence the spin-orbit splittings obviously but having different effects for different hyperons. For the Λ and $\Xi^{0,-}$ hyperons, the ωYY tensor potentials reduce the spin-orbit splittings, while for the $\Sigma^{+,0,-}$ hyperons they are increased. Especially, for the $\Xi^{0,-}$ hyperons, the level ordering is inverted by large ωYY tensor potential.

References:

[1] DANYSZ M, PNIEWSKI J. Philos Mag, 1953, **44**: 348.
[2] HASHIMOTO O, TAMURA H. Prog Part Nucl Phys, 2006, **57**: 564.
[3] GAL A, HUNGERFORD E V, MILLENER D J. Rev Mod Phys, 2016, **88**: 035004.
[4] NAGAE T. Prog Theor Phys Suppl, 2010, **185**: 299.
[5] HAO J, KUO T T S, REUBER A, *et al*. Phys Rev Lett, 1993, **71**: 1498.
[6] HIYAMA E, MOTOBA T, RIJKEN T A, *et al*. Prog Theor Phys Suppl, 2010, **185**: 1.
[7] SCHAFFNER-BIELICH J. Nucl Phys A, 2008, **804**: 309.
[8] XING X Y, HU J N, SHEN H. Phys Rev C, 2017, **95**: 054310.
[9] SUN T T, XIA C J, ZHANG S S, *et al*. Chin Phys C, 2018, **42**: 025101.
[10] HAYANO R S, ISHIKAWA T, IWASAKI M, *et al*. Phys Lett B, 1989, **231**: 355.
[11] PROWSE D J. Phys Rev Lett, 1966, **17**: 782.
[12] DANYSZ M, GARBOWSKA K, PNIEWSKI J, *et al*. Nucl Phys, 1963, **49**: 121.
[13] AOKI S, BAHK S Y, CHUNG K S, *et al*. Prog Theor Phys, 1991, **85**: 1287.
[14] KHAUSTOV P, ALBURGER D E, BARNES P D, *et al*. Phys Rev C, 2000, **61**: 054603.
[15] AOKI S, BAHK S Y, CHUNG K S, *et al*. Prog Theor Phys, 1993, **89**: 493.
[16] NAKAZAWA K, ENDO Y, FUKUNAGA S, *et al*. Prog Theor Exp Phys, 2015, **2015**: 033D02.
[17] MOTOBA T, BANDŌ H, IKEDA K. Prog Theor Phys, 1983, **70**: 189.
[18] HIYAMA E, KAMIMURA M, YAMAMOTO Y, *et al*. Phys Rev Lett, 2010, **104**: 212502.
[19] ZHOU X R, SCHULZE H J, SAGAWA H, *et al*. Phys Rev C, 2007, **76**: 034312.
[20] LU B N, ZHAO E G, ZHOU S G. Phys Rev C, 2011, **84**: 014328.
[21] HIYAMA E, KAMIMURA M, MOTOBA T, *et al*. Phys Rev C, 1996, **53**: 2075.
[22] ZHOU X R, POLLS A, SCHULZE H J, *et al*. Phys Rev C, 2008, **78**: 054306.
[23] LÜ H F, MENG J. Chin Phys Lett, 2002, **19**: 1775.
[24] SONG C Y, YAO J M. Chin Phys C, 2010, **34**: 1425.
[25] LU W L, LIU Z X, REN S H, *et al*. J Phys G: Nucl Part Phys, 2017, **44**: 125104.
[26] REN S H, SUN T T, ZHANG W. Phys Rev C, 2017, **95**: 054318.
[27] SUN T T, LU W L, ZHANG S S. Phys Rev C, 2017, **96**: 044312.
[28] BANDŌ H, MOTOBA T, ŽOFKA J. Int J Mod Phys A, 1990, **05**: 4021.
[29] GAL A, SOPER J M, DALITZ R H. Ann Phys (N.Y.), 1971, **63**: 53.
[30] MILLENER D J. Nucl Phys A, 2008, **804**: 84.
[31] ISAKA M, KIMURA M, DOTE A. Phys Rev C, 2011, **83**: 044323.
[32] BROCKMANN R, WEISE W. Phys Lett B, 1977, **69**: 167.
[33] MAREŠ J, JENNINGS B K. Phys Rev C, 1994, **49**: 2472.
[34] SHEN H, YANG F, TOKI H. Prog Theor Phys, 2006, **115**: 325.
[35] LIU Z X, XIA C J, LU W L, *et al*. Phys Rev C, 2018, **98**: 024316.
[36] WIRTH R, GAZDA D, NAVRÁTIL P, *et al*. Phys Rev Lett, 2014, **113**: 192502.
[37] SERT B D, WALECKA J D. Adv Nucl Phys, 1986, **16**: 1.
[38] MENG J, ZHOU S G. J Phys G: Nucl Part Phys, 2015, **42**: 093101.
[39] SUN T T. Sci Sin Phys Mech Astron, 2016, **42**: 012006. (in Chinese)
[40] BRÜCKNER W, FAESSLER M A, KETEL T J, *et al*. Phys

Lett B, 1978, **79**: 157.
[41] LONG W H, MENG J, VAN GIAI N, *et al*. Phys Rev C, 2004, **69**: 034319.
[42] SUN T T, HIYAMA E, SAGAWA H, *et al*. Phys Rev C, 2016, **94**: 064319.
[43] FORTIN M, AVANCINI S S, PROVIDÊNCIA C, *et al*. Phys Rev C, 2017, **95**: 065803.
[44] NAGAE T, MIYACHI T, FUKUDA T, *et al*. Phys Rev Lett, 1998, **80**: 1605.
[45] DOVER C B, GAL A. Prog Part Nucl Phys, 1984, **12**: 171.
[46] NAGELS M M, RIJKEN T A, DE SWART J J. Phys Rev D, 1975, **12**: 744.

相对论平均场理论对 Λ, Ξ 和 Σ 超核的研究

刘子鑫[1]，夏铖君[2]，孙亭亭[1,†]

(1. 郑州大学物理工程学院，郑州 450001；
2. 浙江大学宁波理工学院，浙江 宁波 300071)

摘要： 基于相对论平均场理论，系统地研究了单 Λ，Ξ 和 Σ 超核，超子-核子相互作用通过拟合实验数据以及参照之前理论工作来确定。以 ^{16}O 为核芯，通过加入不同类型超子(Λ，$\Xi^{0,-}$ 和 $\Sigma^{+,0,-}$)，比较了超子的平均势场和单粒子能级，并研究了对核芯的杂质效应。整体上看，Λ 和 Ξ^0 超子在大块性质上类似；Ξ^0 超子平均势场最浅；库仑相互作用对于带电超子 Ξ^-，Σ^+ 和 Σ^- 非常重要。作为杂质，原子核中加入超子会使整个体系更束缚。然而，不同超子对原子核的半径有不同效应。此外，讨论了 ωYY 张量耦合，发现其对超子的能级劈裂有显著影响，甚至导致 Ξ 超子中出现能级反转现象。

关键词： 超核；超子-核子相互作用；ωYY 张量耦合；相对论平均场模型

收稿日期： 2018-09-23； **修改日期：** 2018-11-03
基金项目： 国家自然科学基金资助项目(11505157, 11705163)；郑州大学物理学科推进计划(32410017)
† **通信作者：** 孙亭亭，E-mail: ttsunphy@zzu.edu.cn。